ENHANCED LASER SCATTERING AND BREMSSTRAHLING EMISSION FROM NONTHERMAL THETA-PINCH PLASMAS

Howard M. Stainer

Johns Hopkins University
Silver Spring, Maryland

October 1972

TG 1199
OCTOBER 1972
Copy No. 25

Technical Memorandum

ENHANCED LASER SCATTERING AND BREMSSTRAHLUNG EMISSION FROM NONTHERMAL THETA-PINCH PLASMAS

by HOWARD M. STAINER

THE JOHNS HOPKINS UNIVERSITY • APPLIED PHYSICS LABORATORY

UNCLASSIFIED
Security Classification

DOCUMENT CONTROL DATA - R & D

(Security classification of title, body of abstract and indexing annotation must be entered when the overall report is classified)

1. ORIGINATING ACTIVITY (Corporate author)	2a. REPORT SECURITY CLASSIFICATION
The Johns Hopkins University Applied Physics La. 8621 Georgia Ave. Silver Spring, Md. 20910	UNCLASSIFIED 2b. GROUP na

3. REPORT TITLE

Enhanced Laser Scattering and Bremsstrahling Emission from Nonthermal Theta-Pinch Plasmas

4. DESCRIPTIVE NOTES (Type of report and inclusive dates)

Technical Memorandum

5. AUTHOR(S) (First name, middle initial, last name)

Howard M. Stainer

6. REPORT DATE	7a. TOTAL NO. OF PAGES	7b. NO. OF REFS
October 1972	57 61	22

8a. CONTRACT OR GRANT NO.	9a. ORIGINATOR'S REPORT NUMBER(S)
N0001"-"2-C-4401	
b. PROJECT NO.	TG 1199
c.	9b. OTHER REPORT NO(S) (Any other numbers that may be assigned this report)
d.	

10. DISTRIBUTION STATEMENT

Distribution of this report is unlimited.

11. SUPPLEMENTARY NOTES	12. SPONSORING MILITARY ACTIVITY
	NAVORDSYSCOM

13. ABSTRACT

We are investigating the conditions under which enhanced scattering of far-IR laser radiatio ($\lambda = 337\mu$) can be obtained from theta-pinch plasmas. The enhanced scattering cross section results from large electron density fluctuations generated by nonthermal electrons in the plasma. The scattering cross section is derived from kinetic theory using "rigid rotor" distributions to model the specific theta-pinch plasma and the conditions under which it can become greatly enhanced are examined. Three types of bremsstrahlung – free-free, magnetic wave-wave, and nonmagnetic wave-wave – are discussed and the power produced by each kind computed and compared to the scattered power. For typical HCN laser power densities of the order of 10 watts/cm^2, the bremsstrahlung considerably exceeds the scattered power in both the wideband (over all frequencies) and narrowband receiver cases. Additional calculations indicate that an experiment with the more powerful CO_2 laser ($\lambda = 10.6\mu$) would be more likely to succeed.

DD FORM 1 NOV 1473

UNCLASSIFIED
Security Classification

14. KEY WORDS

Theta-pinch Plasmas
Nonthermal Electrons
Electron Density Fluctuations
Far IR and CO_2 Lasers
Enhanced Laser Scattering
Enhanced Bremsstrahlung

TG 1199
OCTOBER 1972

Technical Memorandum

ENHANCED LASER SCATTERING AND BREMSSTRAHLUNG EMISSION FROM NONTHERMAL THETA-PINCH PLASMAS

by HOWARD M. STAINER

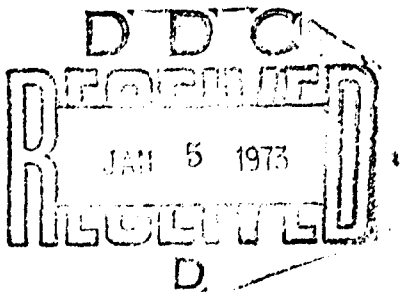

THE JOHNS HOPKINS UNIVERSITY • APPLIED PHYSICS LABORATORY
8621 Georgia Avenue • Silver Spring, Maryland • 20910
Operating under Contract N00017-72-C-4401 with the Department of the Navy

THE JOHNS HOPKINS UNIVERSITY
APPLIED PHYSICS LABORATORY
SILVER SPRING, MARYLAND

ABSTRACT

We are investigating the conditions under which enhanced scattering of far-infrared laser radiation ($\lambda = 337\mu$) can be obtained from theta-pinch plasmas. The enhanced scattering cross section results from large electron density fluctuations generated by nonthermal electrons in the plasma. The scattering cross section is derived from kinetic theory using "rigid rotor" distributions to model the specific theta-pinch plasma and the conditions under which it can become greatly enhanced are examined. Three types of bremsstrahlung – free-free, magnetic wave-wave, and nonmagnetic wave-wave – are discussed and the power produced by each kind computed and compared to the scattered power. For typical HCN laser power densities of the order of 10 watts/cm^2, the bremsstrahlung considerably exceeds the scattered power in both the wideband (over all frequencies) and narrowband receiver cases. Additional calculations indicate that an experiment with the more powerful CO_2 laser ($\lambda = 10.6\mu$) would be more likely to succeed.

THE JOHNS HOPKINS UNIVERSITY
APPLIED PHYSICS LABORATORY
SILVER SPRING MARYLAND

CONTENTS

CONTENTS (cont'd)

ILLUSTRATIONS

TABLES

1. INTRODUCTION

The Plasma Dynamics Group (CPR) is using far-infrared lasers (337μ to 119μ) as tools for plasma diagnostic work. One experiment currently under consideration is the scattering of laser-produced 337μ radiation from a theta-pinch plasma. Because of the background noise level involved (bremsstrahlung, etc.) in laser scattering from such theta-pinch plasmas, it is necessary to obtain considerable enhancement over the thermal scattering cross section. This report will examine some conditions under which we expect to obtain this enhancement.

We are considering the incoherent scattering of electromagnetic radiation from electron density fluctuations as in Refs. 1 and 2. The enhanced scattering cross section depends on the existence of enhanced levels of electron density fluctuations that in turn can be produced only by a plasma with a nonthermal electron component.

The incoming radiation interacts with the electron density fluctuations and is absorbed by the plasma. The oscillating electrons generating the density fluctuations then reradiate the scattered radiation. When the propagating oscillations or plasma waves (that are induced by the beating between the incoming and outgoing frequencies and wavenumbers) have the same direction and phase velocity as those generated by the nonthermal density fluctuations, then resonance occurs and a substantial enhancement of the scattering cross section is obtained.

In a thermal plasma the ion and electron distribution functions, f, are Maxwellian. If we arbitrarily pick out a single electron traveling at some velocity, v_o, then this electron generates a Cerenkov wake or train of longitudinal plasma oscillations behind it with phase velocities ω/k between 0 and v_o. In a thermal plasma ($\partial f/\partial v < 0$) there are always more particles with velocities just less than some given velocity than there are particles with

velocities just greater than this given arbitrary velocity. Thus an electrostatic wave propagating through the plasma with this phase velocity will gain some energy from the slightly faster particles but will lost more energy to the more numerous slower particles. In short, the wave will be damped with the magnitude of the damping proportional to $\partial f/\partial v$. This is one usual way of explaining Landau damping (see, for example, Montgomery and Tidman, Appendix B (Ref. 3). Thus, the longitudinal plasma oscillations generated by our test electron will be absorbed by the Maxwellian plasma. In this way, a balance is struck between emitted and absorbed longitudinal plasma oscillations that determines the low amplitude level of the thermal electron density fluctuations.

In a nonthermal plasma, however, we can have a region in velocity space where $\partial f/\partial v$ is almost zero (see Fig. 1). This can be caused, for example, by having a number of high-speed electrons drift through the background plasma (if V_e is the thermal speed of the background electrons, $V_e^2 = KT/m_e$, then $V_d >$ several V_e, where V_d is the drift velocity of the high-speed electrons). The high-speed electrons generate (as before) their electrostatic Cerenkov plasma oscillations. Now, however, there is the critical difference that very little absorption take place for those oscillations having phase velocities within the $\partial f/\partial v \approx 0$ region of velocity space. The peak electrostatic field amplitudes become quite large and hence the amplitudes of the corresponding electron density fluctuations become much larger than for the thermal case.

Under these conditions, therefore, the scattering cross section becomes greatly enhanced. In a similar way, we will see later that certain types of bremsstrahlung involving collisions between traveling plasma oscillations or waves will also be greatly enhanced over thermal values.

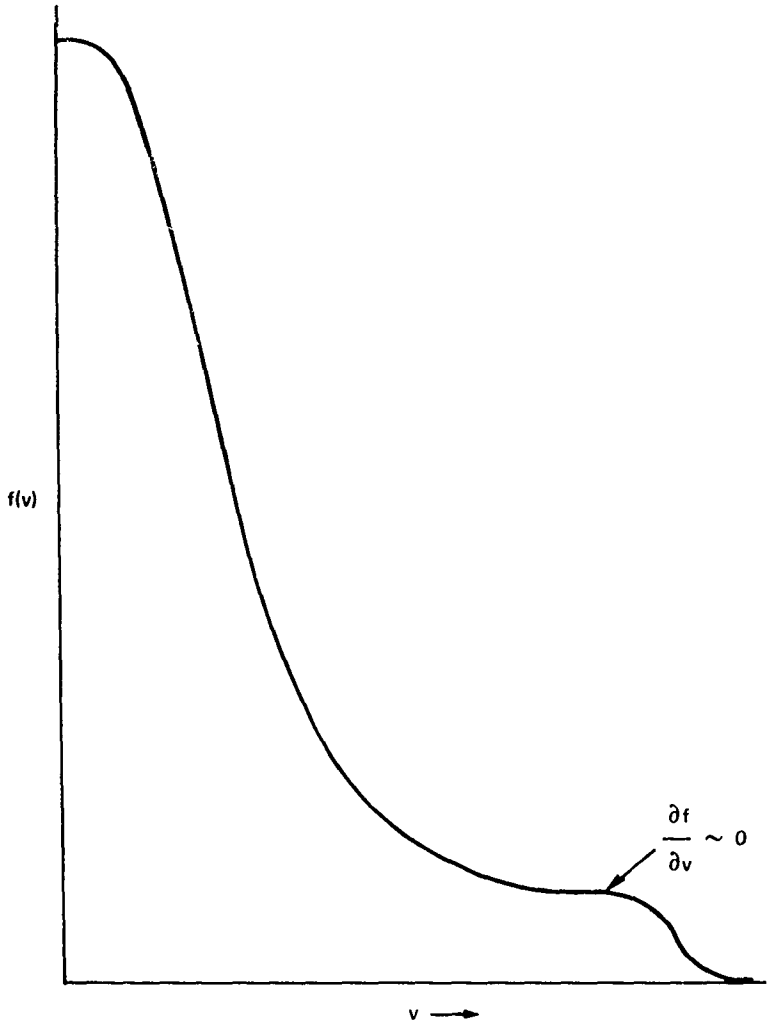

Fig. 1 SCHEMATIC OF VELOCITY DISTRIBUTION WHERE $\partial f/\partial v$ IS ALMOST ZERO

2. THEORY

We are considering the standard situation (Refs. 1 and 3) in which an incident plane wave of frequency Ω_o is scattered by the plasma through some angle and the scattered radiation emerges at the frequency ω. The differential cross section σ (per unit frequency interval and per unit solid angle) is given as:

$$\sigma(\bar{\omega}) = r_o^2 \, S\left(\vec{K} - \frac{\omega}{c}\vec{N},\ \omega - \Omega_o\right) \qquad (1)$$

where S is the spectral density, $\bar{\omega}$ is $(\omega - \Omega_o)/\Omega_o$, and r_o – the classical electron radius – is e^2/mc^2. $\vec{K}$ is the wave vector of the incoming radiation and $\vec{N}$ is the unit vector in the direction of the scattered radiation. We will see later that the frequency condition for enhancement is that $|\omega - \Omega_o| \approx \omega_p$ where ω_p is the plasma frequency ($\omega_p^2 = 4\pi e^2 n/m_e$). In the case where $\Omega_o >> \omega_p$ then $|\omega - \Omega_o| << \Omega_o$ and we can write $\vec{k} = \vec{K} - (\omega/c)\vec{N} \approx \vec{K} - (\Omega_o/c)\vec{N}$.

The dominant term in S is that for the electrons, where S is given, for example, by Eq. (16) of Rosenbluth and Rostoker (Ref. 1). It is convenient to use the notation of Tidman and Dupree (Ref. 4) and we find that:

$$S_{ee}(\vec{k}, \omega) = \frac{2\mathrm{Re}(U_e)}{|D|^2}\,|1 - L_i^2| + \frac{2\mathrm{Re}(U_i)}{|D|^2}\,L_e^2 \qquad (2)$$

where the arguments on the right-hand side of Eq. (2) are $(\vec{k}, i\omega)$.

If we use a "weak" field expansion (Ref. 5) where $\Omega_\alpha^2 << \omega_p^2$ ($\Omega_\alpha = e|B_o|/m_\alpha c$; α indicates ions or electrons),

then in lowest order U_α and L_α can be defined as in the zero magnetic field case. The roots of the dispersion relation, Re(D) = 0, however, are changed somewhat by the inclusion of the field.

With this in mind, the quantities in Eq. (2) are defined as follows:

$$U_\alpha(\vec{k}, s) \approx \int_{-\infty}^{\infty} d\vec{v} \; \frac{f_\alpha(\vec{v})}{(s + i\vec{k} \cdot \vec{v})} \tag{3}$$

$$L_\alpha(\vec{k}, s) \approx \frac{\omega_\alpha^2}{k^2} \int_{-\infty}^{\infty} d\vec{v} \; \frac{\vec{k} \cdot \frac{\partial f_\alpha}{\partial \vec{v}}}{(s + i\vec{k} \cdot \vec{v})} \qquad \mathrm{Re}(s) > 0 \tag{4}$$

with

$$D(\vec{k}, s) = 1 - \sum_\alpha L_\alpha(\vec{k}, s) \tag{5}$$

Thus, in lowest order we find (Ref. 5) that:

$$\mathrm{Im}\; D(\vec{k}, i\omega) \approx \sum_\alpha \frac{\pi \omega_\alpha^2}{k^2} F_\alpha'(-\vec{k}, \omega/k), \tag{6}$$

$$\mathrm{Re}\; U(\vec{k}, i\omega) \approx \frac{\pi}{k} F_\alpha(-\vec{k}, \omega/k), \tag{7}$$

and

$$\mathrm{Re}\; D(\vec{k}, i\omega) \approx 1 - \frac{\omega_p^2}{\omega^4}\left[\omega^2 + 3(k_\perp^2 V_\perp^2 + k_\parallel^2 V_\parallel^2) + \frac{\Omega_e^2 k_\perp^2}{k^2}\right]. \tag{8}$$

(Only the electron contribution is included in Eq. (8) since $m_i >> m_e$.)

As usual, the reduced distributions, F_a, are defined by:

$$F'_{\alpha}(\vec{k}, u) = \int_{-\infty}^{\infty} d\vec{v}\, f_{\alpha}(\vec{v})\, \delta\left(u - \frac{\vec{k}\cdot\vec{v}}{k}\right) \tag{9}$$

and

$$\int_{-\infty}^{\infty} d\vec{v}\, f_e(\vec{v}) \begin{pmatrix} v_\perp^2 \\ v_\parallel^2 \end{pmatrix} = \begin{pmatrix} 2V_\perp^2 \\ V_\parallel^2 \end{pmatrix} \tag{10}$$

We shall consider frequencies near ω_p and $k < k_D$. Then the spectral density becomes (similarly to Ref. 5):

$$S_{ee}(\vec{k}, \omega \approx \omega_p) \approx \frac{2\mathrm{Re}(U_e)}{|D|^2} \approx 2\mathrm{Re}(U_e) \cdot$$

$$\left\{\left[1 - \frac{\omega_p^2}{\omega^2} - \frac{\omega_p^2\Omega_e^2}{\omega^4}\sin^2\theta_o - \frac{3\omega_p^2}{\omega^4}(k_\perp^2 V_\perp^2 + k_\parallel^2 V_\parallel^2)\right]^2 + [\mathrm{Im}(D)]^2\right\}^{-1}, \tag{11}$$

where θ_o is the angle between $\vec{k}$ and $\vec{B}_o$. This can be written (Ref. 4) as:

$$S_{ee}(\vec{k}, \omega) \approx \frac{2(\pi\omega_p^2/4k)\, F_e(-\vec{k}, \omega/k)}{(\omega \pm \omega_o)^2 + \gamma_L^2} \tag{11a}$$

where γ_L is the Landau damping decrement,

$$\gamma_L = (\pi\omega_p^3/2k^2)\, F_e'(-\vec{k}, \omega/k) = (\omega_p/2)\, \mathrm{Im}(D), \tag{12}$$

and ω_o is the solution of $\mathrm{Re}(D) = 0$, i.e.,

$$\omega_o \approx \left|\omega_p^2 + \Omega_c^2 \sin^2\theta_o + 3(k_\perp^2 V_\perp^2 + k_\parallel^2 V_\parallel^2)\right|^{\frac{1}{2}}, \tag{13}$$

and we have written $\Omega_c = |\Omega_e|$. Thus S_{ee} has a resonance or Lorentzian line shape.

If we wish to consider just the scattering cross section per unit solid angle σ_t, we integrate out the frequency dependence, i.e.,

$$\sigma_t = \int_{-\infty}^{\infty} \sigma(\bar{\omega}) \frac{d\omega}{2\pi} \tag{14}$$

When S_{ee} is integrated to obtain σ_t, we can represent the resonance as a delta function (Refs. 4 and 5). That is, we consider the regime where γ_L is very small but not exactly zero ($\gamma_L = 0$ indicates the onset of instability). Thus we neglect the effects due to finite resonance breadth γ_L to obtain:

$$S_{ee}(|\omega| \approx \omega_p,\ \vec{k} < k_D) \approx \frac{\pi k \omega_o}{\omega_p^2} \frac{F_e(-\vec{k},\ \omega/k)}{|F_e'(-\vec{k},\ \omega/k)|} \left[\delta(\omega-\omega_o) + \delta(\omega+\omega_o)\right] \tag{15}$$

where the prime denotes differentiation with respect to the second variable, ω/k. We will get enhancement only when the arguments of S_{ee} are as indicated in Eq. (15). Thus, from Eq. (1) we require $|\omega - \Omega_o| \approx \omega_p$ and our final expression for S_{ee} is:

$$S_{ee}\left(\vec{K} - \frac{\Omega_o}{c}\vec{N},\ |\omega - \Omega_o| \approx\right.$$

$$\left.\frac{\pi k \omega_o}{\omega_p^2} \frac{F_e\left(\frac{\Omega_o}{c}\vec{N} - \vec{K},\ \frac{(\omega-\Omega_o)}{k}\right)}{\left|F_e'\left(\frac{\Omega_o}{c}\vec{N} - \vec{K}, \frac{(\omega-\Omega_o)}{k}\right)\right|} \left[\delta(\omega-\Omega_o-\omega_o) + (\omega-\Omega_o+\omega_o)\right] \right) \tag{16}$$

Using Eqs. (16) and (1) in Eq. (14) gives us

$$\sigma_t \approx \frac{\omega_o k}{\omega_p} \frac{r_o^2}{2} \left[\frac{F_e\left(\frac{\Omega_o}{c}\vec{N} - \vec{K}, \frac{\omega_o}{k}\right)}{\left|F_e'\left(\frac{\Omega_o}{c}\vec{N} - \vec{K}, \frac{\omega_o}{k}\right)\right|} + \frac{F_e\left(\vec{K} - \frac{\Omega_o}{c}\vec{N}, \frac{\omega_o}{k}\right)}{\left|F_e'\left(\vec{K} - \frac{\Omega_o}{c}\vec{N}, \frac{\omega_o}{k}\right)\right|} \right] \qquad (17)$$

In the second term of Eq. (17) we have used the symmetry of Eq. (9), i.e., $F_\alpha(\vec{k}, u) = F_\alpha(-\vec{k}, -u)$.

Equation (17) clearly indicates that F_e' must become very small to give significant enhancement. A thermal or Maxwellian plasma will not yield the desired result; a nonthermal high-energy component of electrons is required. As we have been, the physical mechanism is simply that the balance (present in a thermal plasma) between emission and absorption of electrostatic oscillations is disrupted by the presence of the high-speed electrons. This lack of balance (i.e., enhanced emission coupled with greatly reduced absorption) then leads to excitation of large amplitude density fluctuations.

3. APPLICATION TO THETA-PINCH PLASMAS

The model we propose to use to approximate the laboratory plasma is an infinitely long theta-pinch plasma with a two-component (the background plus the high-speed electrons) rigid rotor distribution function. The use of the rigid rotor distribution is well established for theta-pinch or cylindrically symmetric plasmas confined by an axial magnetic field (Refs. 6 to 14). In this model:

$$f = f\,[-(\epsilon - \omega_s P_\theta)/T]\,. \tag{18}$$

Here
$$\epsilon = \tfrac{1}{2} m\,(v_r^2 + v_\theta^2 + v_z^2) + q\varphi\,,$$
$$P_\theta = mr\,(v_\theta + q\,A_\theta/mc)\,. \tag{19}$$
and

If the magnetic field is time-independent then the energy ϵ of a charged particle is always a constant of the motion. If this field is also cylindrically symmetric, then the canonical angular momentum P_θ of a charged particle is also a constant of the motion. Thus we construct our solution to the Vlasov equation in a magnetic field from the constants of the motion. A convenient specific function to use is the Maxwellian. To quote from Ref. 8: "The term rigid rotor comes from the fact that the mean velocity of the particles described by Eq. (21) [our Eqs. (18) and (20)] is entirely in the θ direction and is proportional to r with proportionality constant ω_s, as is the motion of a cylindrically symmetric rigid body rotating about its axis with angular velocity ω_s." The rigid rotation model has been applied to high beta theta-pinch plasmas in the collisional regime (Ref. 15) and has also been discussed by Komarov and Fadeev (Ref. 16) for collisionless plasmas. Finally, we note that (Ref. 11): "If one considers the Boltzmann equation with a Fokker Planck collision term, then the only equilibrium solution possible is one with rigid rotation."

The type of distribution function we start with is (after Morse (Ref. 8)):

$$f_e(V_j) = \frac{n(r)}{(2\pi)^{3/2} V_j^3} \exp\left\{-\frac{1}{2V_j^2}\left[v_r^2 + v_z^2 + (v_\theta - \omega_j r)^2\right]\right\}, \quad (20)$$

where j is an index denoting the background or high-speed electrons and

$$n(r) = n_o \operatorname{sech}^2\left(\frac{r^2 - r_1^2}{r_o^2}\right) \Big/ \operatorname{sech}^2\left(\frac{-r_1^2}{r_o^2}\right), \quad (21)$$

where r_1 and r_o are constants; r_o is the characteristic dimension of the plasma; and if $r_1^2 > 0$, then r_1 is the radius at which the maximum density occurs.

One case Morse (Ref. 8) discusses is that of a plasma with small net angular momentum where $\omega_e m_e \approx -\omega_i m_i$ and the electrons carry most of the diamagnetic current. We shall use this case to describe our theta-pinch plasma and we propose that

$$f_e \approx (1 - \delta) f_e(V_e) + \delta f_e(V_E) \quad (22)$$

where δ measures the fraction of high-speed electrons ($0 < \delta \ll 1$), V_e is the thermal velocity of the background electrons, and V_E is the thermal velocity of the high-speed or energetic electrons. If we wrote Eq. (22) out in full using Eq. (20), we would note that the high-speed electrons drift through the background plasma in the θ direction with a drift speed V_d given by $\omega_E r$ (where r is the distance from the axis of symmetry) since $\omega_E \gg \omega_e$.

We use Eqs. (20) and (22) in Eq. (9) to find that

$$F_e(\vec{k},u) = \frac{(1-\delta)n(r)}{(2\pi)^{\frac{3}{2}} V_e} \exp\left[-\frac{1}{2V_e^2}\left(u - \frac{k_\theta \omega_e r}{k}\right)^2\right] \qquad (23)$$

$$+ \frac{\delta n(r)}{(2\pi)^{\frac{3}{2}} V_E} \exp\left[-\frac{1}{2V_E^2}\left(u - \frac{k_\theta \omega_E r}{k}\right)^2\right]$$

We insert Eq. (23) in Eq. (17), using the following definitions:

$$\varkappa = 2\omega_p^2/k^2 V_e^2 r_o^2 ,$$

$$a = \omega_o/(2)^{\frac{1}{2}} k V_e ,$$

$$b = \omega_E r\left(\frac{\Omega_o}{c} N_\theta - K_\theta\right)/\omega_o = \omega_E r q_\theta/\omega_o , \text{ and} \qquad (24)$$

$$d = \omega_e/\omega_E ,$$

to obtain a simplified expression for σ_t. Thus:

$$\varkappa\sigma_t \approx \frac{1 + \frac{\delta}{(1-\delta)}\left(\frac{V_e}{V_E}\right) \exp\left\{-a^2\left[\left(\frac{V_e}{V_E}\right)^2 (1-b)^2 - (1-bd)^2\right]\right\}}{\left|(1-bd) + \frac{\delta}{(1-\delta)}\left(\frac{V_e}{V_E}\right)^3 (1-b) \exp\left\{-a^2\left[\left(\frac{V_e}{V_E}\right)^2 (1-b)^2 - (1-bd)^2\right]\right\}\right|} \qquad (25)$$

$$+ \frac{1 + \frac{\delta}{(1-\delta)}\left(\frac{V_e}{V_E}\right) \exp\left\{-a^2\left[\left(\frac{V_e}{V_E}\right)^2 (1+b)^2 - (1+bd)^2\right]\right\}}{\left|(1+bd) + \frac{\delta}{(1-\delta)}\left(\frac{V_e}{V_E}\right)^3 (1+b) \exp\left\{-a^2\left[\left(\frac{V_e}{V_E}\right)^2 (1+b)^2 - (1+bd)^2\right]\right\}\right|}$$

From the symmetry of Eq. (25) with respect to b, it is clear that b could just as well be defined as $\omega_E{}^r\,|(\Omega_o/c)N_\theta - K_\theta|$.

4. ENHANCED SCATTERING RESONANCE

We now wish to examine the conditions under which the right-hand side of Eq. (25) can become very large. We first note that if $\delta = 0$, the purely thermal case, then $\varkappa\sigma_t = 2/(1 - b^2d^2)$. This will be our standard of reference. In the cases we will consider, b is never much greater than 1.0 and d is always 0.1 or smaller; thus for all practical purposes, $\varkappa\sigma_t \approx 2$ in the thermal case.

The right-hand side of Eq. (25) can become very large if either one or both of the denominators becomes very small, or one or both of the numerators becomes very large. The two points at which this happens are when the denominator vanishes and when b equals 1. (These possibilities occur only with the first term where b is preceded by a minus sign.) We will see later that while the spike produced by the vanishing denominator is infinite in amplitude, it is extremely narrow with respect to b (see the Appendix). Thus, the total energy in the fluctuations and the power reradiated is finite. This situation is similar to that described by Tidman and Dupree (Ref. 4, Section 5), where they find that the spectral density S diverges. However, when one wavenumber, k, first becomes unstable, they found: "...an uninteresting change in the bremsstrahlung – i.e., there is no spectacular increase in the emission...." They determined that the resonance must be quite broad for a detectable increase: "For enhanced emission we require that a range of wavenumbers are bordering on instability – or at least that a range of wavenumbers have an extremely small Landau damping." Hence, for all practical purposes, we consider Eq. (20) as used in Eq. (22) a stable nonthermal distribution. An unstable distribution generating gross instabilities cannot be handled within the framework of our theory. Thus, exceedingly large amplitudes in the density fluctuations invalidate the basic

premise on which the theory is based (Ref. 17), namely, that the nonthermal fluctuation level is considerably less than the thermal fluctuation level divided by the plasma discreteness parameter Δ ($\Delta^{-1} = n_o \lambda_D^3$, where n_o is the average density and λ_D is the Debye length).

A staple resonance does occur for b = 1. If we consider only those cases for which $bd \ll 1$ and $a^2 \gg 1$, for example, then we find that the dominant term in Eq. (25) can be written as:

$$\chi\sigma_t \approx \frac{\delta}{(1-\delta)} \frac{V_e}{V_E} \exp(a^2) . \qquad (26)$$

Thus we see that for sufficiently large values of a (and to a lesser degree of importance, δ and V_e/V_E), we can get orders of magnitude enhancement over the thermal value of 2.

5. DISCUSSION

Broadness of Scattering Resonance

As a starting point, we arbitrarily use the following set of numbers: $\delta = 10^{-6}$, $V_E = 10\ V_e$, $a = 6$, and $d = 10^{-2}$. Exactly at resonance ($b = 1$) the enhancement over thermal is 2.1×10^8. This resonance is quite sharp in terms of full width at half maximum. For example, a change in b (Δb) of $\pm\ 0.01\%$ drops the enhancement factor to 5×10^5. We should note, however, that the further decline in enhancement drops rapidly as $|\Delta b|$ becomes larger (the resonance line is essentially symmetric about $b = 1$, apart from the aforementioned narrow spike). At Δb's of 1% and 20%, we still have enhancement factors of approximately 5×10^3 and 3×10^2, respectively. We also note that since ω_o is a very large frequency ($\sim 2 \times 10^{12}$ Hz) we still get enhancement factors of 5×10^5 or better over a bandwidth of 200 MHz on each side of the resonance.

Sensitivity to Parameter Changes

The parameter, a, given in Eq. (24) is proportional to the phase velocity of the plasma oscillation over the thermal velocity of the background electrons. At resonance ($b = 1$), and in the backscattering case where $\vec{N}$ and $-\vec{K}$ are in essentially the same direction along a chord a distance R_o from the axis and $k = 2\,\Omega_o/c$, then we have:

$$\omega_o = 2\omega_E \left(\frac{\Omega_o R_o}{c} \right). \tag{27}$$

In this case, $a^2 = \frac{1}{2}\,(V_d/V_e)^2$, where $V_d\ (= \omega_E R_o)$ is the drift velocity of the high-speed electrons and V_e is the thermal velocity of the background electrons.

If we look at Eq. (25), we see that it is a function of four variables. These are: δ, the fraction of high-

speed electrons; V_E/V_e, the ratio of the thermal velocities; b, the resonance factor; and a, as discussed above. These parameters were varied as follows:

1. $\delta/(1-\delta) = 10^{-7}, 10^{-6}, 10^{-5}, 10^{-4}$
2. $V_E/V_e = 1, 3, 5, 6, 10$
3. a = 1, 2, 3, 4, 5, 6
4. b = 1, 0.99995, 0.9999, 0.9990, 0.9901, 0.9091

To summarize the results, in all cases studied, significant enhancement occurred only when a = 5 or 6. At most, a = 4 led to enhancements of about 90. Not surprisingly, the enhancement factors were more or less proportional to δ with the largest value for $\delta/(1-\delta) = 10^{-4}$. A small value of V_E increased the magnitude of the resonance but sharpened it considerably. Thus, for a = 6, $V_E/V_e = 1$ gave a b = 1 resonance 10 times larger than $V_E/V_e = 10$. At b = 0.999 (off resonance), however, the $V_E/V_e = 10$ case yielded 100 times the enhancement. We find, therefore, that the enhancement is not particularly sensitive to δ or V_E/V_e although large values of both are desirable. In all situations studied, the "wings" of the enhancement profile are quite wide and flat; here the magnitude out in the wings is affected by the V_E/V_e ratio as noted above.

The critical factor then is a. We will not get significant enhancement (> 100) unless we have a > 4.

Some Practical Considerations

The natural frequency of the plasma ω_o (given by Eq. (13)) is not very different from the plasma frequency ω_p which is a function of the density. Thus, if resonance conditions are met at a particular point in the plasma, then the density variation away from this point may "detune" the resonance.

If the radiation enters the plasma along a chord (the backscattering case) located a distance R_o from the axis, then we can calculate the distance of any point along the chord to the axis (see Fig. 2).

The distance of the point to the axis, ρ_1, is given by:

$$\rho_1 = \left| \rho_o^2 + s^2 \quad 2s \left(\rho_o^2 - R_o^2\right)^{\frac{1}{2}} \right|^{\frac{1}{2}}, \tag{28}$$

where ρ_o is the radius of the plasma, and s is the distance along the chord from the surface (Fig. 2). Thus ρ_1 ranges from a maximum of ρ_o to a minimum of R_o. If R_o is large fraction of ρ_o, the variation of ρ_1 can be quite slow. In addition, ω_o will vary slightly slower than $\sqrt{n}$ so that the variation of ω_o along a large R_o chord need not be too fast. It might also be possible to have a geometrical arrangement such that rq_θ decreases in about the same proportion as ω_o decreases (Eq. (24)).

Forward scattering (i.e., angle between source and receiver > 90°) appears to impose undue restrictions on the resonance condition by making q_θ quite small. For example, in the worst case when the receiver is in a direct line with the laser, V_d needs to be of the order of c. We do not believe that this occurs in the plasma in the first place, and in the second place, our treatment has been strictly non-relativistic. As the receiver is swung around the plasma towards the backscattering region, q_θ increases, thereby relaxing the restriction that V_d = c and making the resonance condition more achievable.

One geometry that gives poor results is equal-angle scattering. That is, the source and receiver are located at equal angles from the vertical reference line, with the point of intersection on the vertical line (see Fig. 3). This geometry gives essentially the same result as the worst case cited above ($V_d \approx c$) and hence no enhancement.

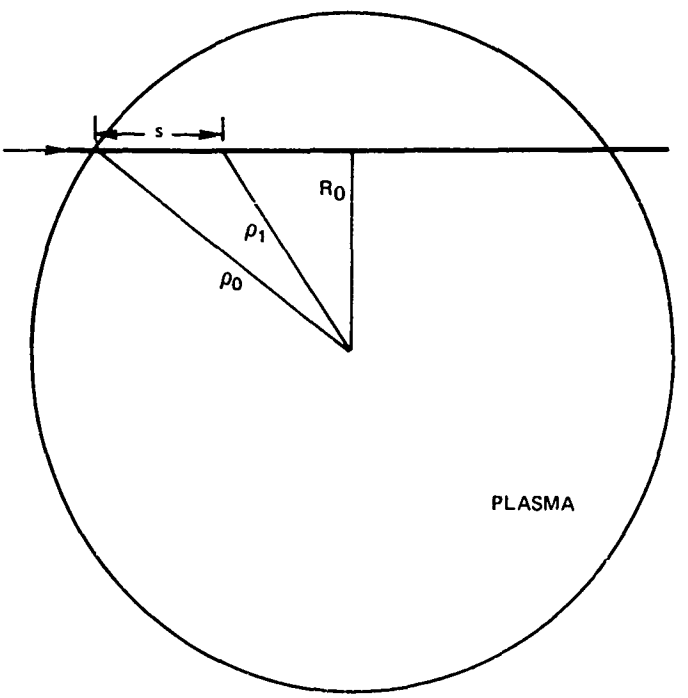

Fig. 2 CHORD GEOMETRY SHOWING DISTANCE FROM AXIS $\rho 1$ AS A FUNCTION OF DISTANCE ALONG THE CHORD s

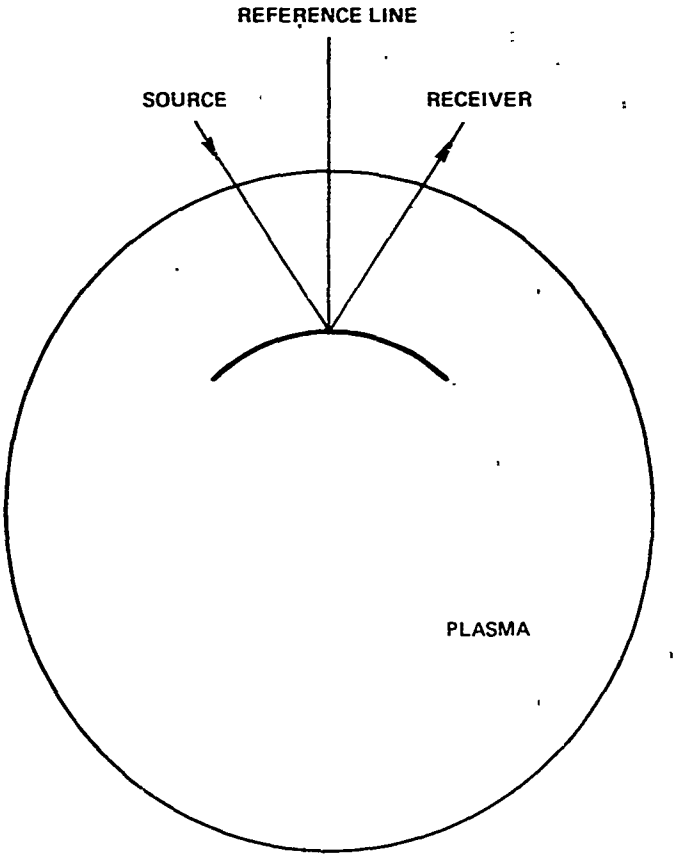

Fig. 3 EQUAL ANGLE GEOMETRY: THETA COMPONENTS ESSENTIALLY CANCEL OUT TO GIVE NO ENHANCEMENT

A geometry that seems promising is shown in Fig. 4. This might be called (case B) equal-angle scattering about a chord (i.e., a line that does not intersect the axis of the plasma). In Fig. 3 geometry, the theta-components of the incident and scattered radiation wave vectors almost cancel; in Fig. 4 geometry (case B), the vectors add. We note that the theta components for cases A and C are much smaller. Thus, the Fig. 4 geometry has the advantage that q_θ decreases as r increases, thereby enabling the resonance condition to be maintained in a larger volume of the plasma.

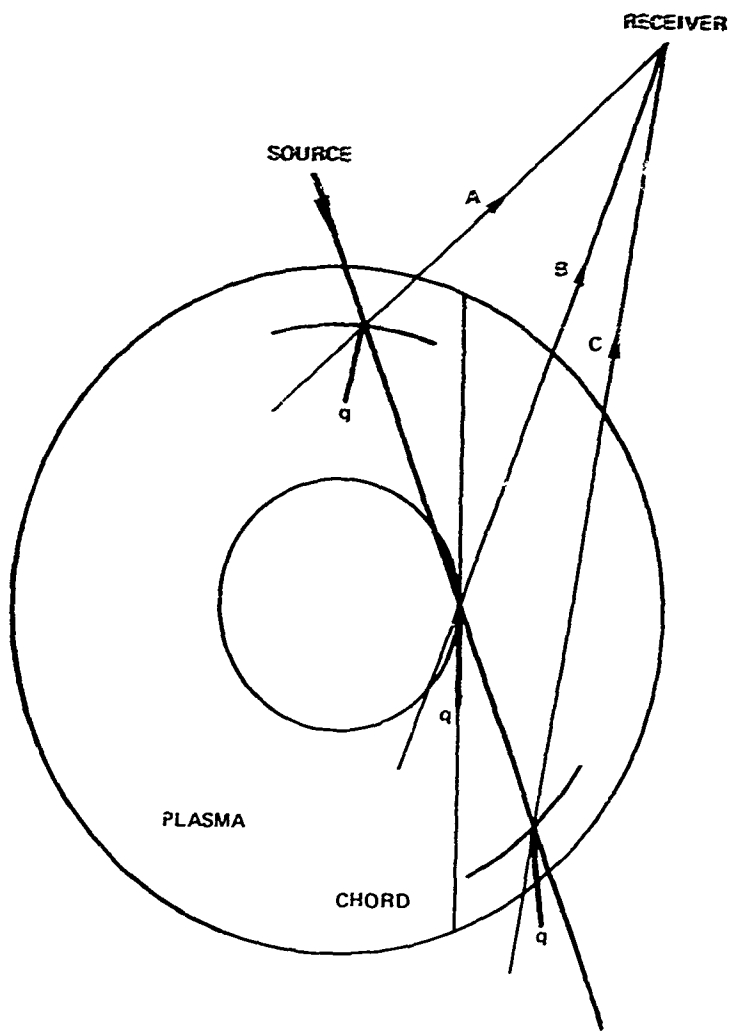

Fig. 4 GEOMETRY FAVORABLE FOR ENHANCEMENT (CASE B)

6. BREMSSTRAHLUNG

Bremsstrahlung (or braking radiation) is the electromagnetic radiation emitted whenever a charged particle is accelerated. Because of its small mass, the electron is nearly always the particle under consideration.

When an electron emits a photon in an electron-ion collision and the heavy ion absorbs the momentum, the electron must decrease its energy (Spitzer, Ref. 18). If the electron remains free, such transitions are called free-free. The usual formula for free-free bremsstrahlung (Ref. 18 and Glasstone and Lovberg, Ref. 19) is obtained by summing the contribution due to single electrons by giving the electrons a Maxwellian distribution of velocities.

If we wish to consider "clumps" of electrons in a plasma interacting in a coherent or cooperative way with clumps of ions or other clumps of electrons, then we obtain wave-wave bremsstrahlung. Some authors (e.g., Ref. 20) refer to this radiation as anomalous bremsstrahlung. Wave-wave bremsstrahlung is produced by collisions between two plasma waves or traveling oscillations. A collision between an electron plasma oscillation (EPO) and an ion plasma oscillation (IPO) will produce bremsstrahlung at essentially the electron plasma frequency (the ion plasma frequency is down by a factor of about 43). Similarly, collisions between two EPO's will produce bremsstrahlung at twice the electron plasma frequency (see, for example, Refs. 4 and 5).

One problem that arises in these scattering experiments then is the noise due to bremsstrahlung. A considerable enhancement in the scattering cross section is needed to handle the noise due to the free-free thermal bremsstrahlung. Nonthermal or anomalous bresmstrahlung is also troublesome since the same basic mechanism

(colliding plasma oscillations) creates both the enhanced electron density fluctuations leading to the enhanced scattering cross section and the nonthermal bremsstrahlung.

The work by Chin-Fatt and Griem (Ref. 20) on nonthermal bremsstrahlung from theta-pinch plasmas is but one reference supporting the theory of Tidman and Dupree (Ref. 4) that colliding longitudinal plasma waves generate electromagnetic radiation. Having calculated that a slab of thermal helium plasma 5 cm thick, with $n_e = n_i = 5 \times 10^{14}$ cm^{-3} and $T_e = 50$ eV, emits less than 10^{-6} W cm^{-2} sr^{-1}/cm^{-1}, Chin-Fatt and Griem (Ref. 20) find that their measured peak intensities are about three orders of magnitude larger. In their case, then, the anomalous or collective bremsstrahlung is dominant over the free-free. The inference is strong that the theta-pinch plasma used in Ref. 20 would also have an enhanced scattering cross section; it certainly has some nonthermal electrons.

In Ref. 20 there is a statement that "...even a thermal plasma has a spectrum of plasma waves in the approximate frequency range $\omega_p \leq \omega \leq 1.4\,\omega_p$..." This implies that a nonthermal plasma may have an even broader spectrum. In any case, the figures for the fundamental and first harmonic with a central density of 10^{16} cm^{-3} indicate a range of 119 to 334μ for this enhanced radiation. Thus, if we are considering plasma puffs of perhaps 2×10^{16} cm^{-3} central density or more, with lower densities away from the core, this rather critical wavelength range of 119 to 337μ is quite thoroughly blanketed.

The ideal situation, of course, would be to have the incident frequency $\Omega_o >$ several ω_p. Then the scattered radiation would be clearly distinguishable from the collective bremsstrahlung and the enhancement in the scattering cross section would be needed only to increase the signal over the thermal bremsstrahlung noise. Unfortunately, experimental limitations may completely preclude this simple theoretical suggestion. Thus, we must investigate

these two simultaneous manifestations (enhanced scattering and anomalous bremsstrahlung) of the plasma's nonthermal nature and consider situations where Ω_o is not greater than several ω_p.

For a given level of electron density fluctuations, there will be a given amount of bremsstrahlung power emitted and a given scattering cross section. On the other hand, the scattered power will always be linearly proportional to the incident power (we are only considering those cases where the low-power laser does not perturb the plasma) with the constant of proportionality determined by the plasma characteristics. Clearly, for ary given plasma, there will be some minimum incident laser power required for the scattered signal to be greater than the bremsstrahlung and we will determine this threshold. (It is always possible, of course, that some kind of sophisticated processing or coding could be employed (using laser modulation, perhaps) to enable a signal-to-noise ratio of less than 1 to be used, but it is not very likely. The transient nature of the plasma puff and the normally pulsed operation of the infrared laser would appear to make this rather difficult. There is the possibility, however, that the technique of narrow-banding the detector would help to pull the scattered signal up above the noise. In this regard, see Section 7.)

Free-Free Bremsstrahlung

The expression for free-free bremsstrahlung is given in many references. Two of these are Spitzer (Ref. 18) and Glasstone and Lovberg (Ref. 19). From Ref. 19 we have:

$$P_{br} = 5.35 \times 10^{-31} n^2 T^{\frac{1}{2}} \quad \text{(watts/cm}^3\text{)}, \qquad (29)$$

where T is in keV.

We are interested in directly comparing the bremsstrahlung emission with the scattered signal. We will,

therefore, consider the bremsstrahlung emitted from the illuminated volume of the plasma under the same conditions that lead to the enhanced scattered resonance. It is convenient to replace n^2 with a term proportional to ω_p^4. Under our weak magnetic field assumption ($\Omega_c^2 \ll \omega_p^2$), we have:

$$\omega_p^2 \approx \omega_p^2 + 3k^2 V_e^2 . \qquad (30)$$

In the backscattering case, $k = 2\Omega_o/c$ and Eq. (27) applies ($\omega_o = 2\omega_E \Omega_o R_o/c$). Combining all these relationships, we find that:

$$\omega_p \approx 2\left(\frac{V_e}{c}\right)\Omega_o (A^2 - 3)^{\frac{1}{2}} , \qquad (31)$$

where $A = V_d/V_e$. Thus, we can write our final free-free bremsstrahlung expression as:

$$P_{br} = 3.233 \times 10^{-6} (A^2 - 3)^2 \quad (\text{watts/cm}^3) , \qquad (32)$$

where we have taken T = 35 eV ($V_e/c = 1.2 \times 10^{-2}$) and $\Omega_o = 5.6 \times 10^{12}$ Hz.

Magnetic Wave-Wave Bremsstrahlung

We reformulate and modify some of the work of Tidman, Birmingham, and Stainer (Ref. 5) to obtain the bremsstrahlung power emitted – at or near the plasma frequency – per unit solid angle ($d\Omega$), per unit volume, and per unit frequency. Thus, we can write:

$$\frac{d^2 I}{d\Omega d\omega} \approx \frac{e^2 \omega_p^2 \left(\omega^2 - \omega_p^2 \mp \omega_p \Omega_c \cos\psi\right)^{\frac{1}{2}}}{8c^3 (2\pi)^4} \int_{k<k_D} \frac{dk_r\, dk_\theta\, dk_z}{k}$$

$$\left\{1 - \frac{1}{2} \frac{\left(k_r^2 + k_\theta^2\right)}{k^2} \sin^2\psi - \frac{k_z^2}{k^2} \cos^2\psi\right\} \tag{33}$$

$$\left[\frac{F_e(\vec{k}, \omega/k)}{|F_e'(\vec{k}, \omega/k)|} + \frac{F_e(-\vec{k}, \omega/k)}{|F_e'(-\vec{k}, \omega/k)|}\right] \delta(\omega - \omega_o) ,$$

where $\omega_o^2 = \omega_p^2 + 3k^2 V_e^2 + \Omega_c^2 (k_r^2 + k_\theta^2)/k^2$ and ψ is the angle between the magnetic field vector and the direction of the emitted radiation. (We note that for the magnetic calculation we include the Ω_c^2 term in ω_o.)

We perform the integration over ω to get:

$$\frac{dI}{d\Omega} \approx \frac{e^2 \omega_p^2}{8c^3 (2\pi)^4} \int_{k<k_D} \frac{dk_r\, dk_\theta\, dk_z}{k} \left(\omega_o^2 - \omega_p^2 \mp \omega_p \Omega_c \cos\psi\right)^{\frac{1}{2}}$$

$$\left\{1 - \frac{1}{2} \frac{\left(k_r^2 + k_\theta^2\right)}{k^2} \sin^2\psi - \frac{k_z^2}{k^2} \cos^2\psi\right\} \tag{34}$$

$$\left[\frac{F_e\left(\vec{k}, \omega_o/k\right)}{|F_e'\left(\vec{k}, \omega_o/k\right)|} + \frac{F_e\left(-\vec{k}, \omega_o/k\right)}{|F_e'\left(-\vec{k}, \omega_o/k\right)|}\right]$$

Equation (34) can be simplified by noting that the square bracket goes through a resonance and hence can be approximated by an appropriate delta function. Thus, we have:

$$\left[\frac{F_e(\vec{k},\omega_o/k)}{|F_e'(\vec{k},\omega_o/k)|}+\frac{F_e(-\vec{k},\omega_o/k)}{|F_e'(-\vec{k},\omega_o/k)|}\right]\approx\frac{\delta}{(1-\delta)}\frac{k}{k_\theta\omega_{E^r}}\frac{V_e^3}{V_E}\exp\left[\frac{1}{2}\left(\frac{k_\theta\omega_{E^r}}{kV_e}\right)^2\right]\times \delta\left(\frac{\omega_o}{\sqrt{2}kV_e}-\frac{\omega_{E^r}k_\theta}{\sqrt{2}kV_e}\right) \tag{35}$$

and we can perform the integration over k_θ. The result is, if ω_o is considered independent of k_θ in the argument of the delta function,

$$\frac{dI}{d\Omega}\approx\frac{e^2\omega_p^2\delta V_e^{\frac{4}{2}}/2)^{\frac{1}{2}}}{3c^3(2\pi)^{\frac{4}{2}}(1-\delta)V_E\omega_{E^r}}\int_{k<k_D}\frac{kd\,k_r\,dk_z}{\omega_o}\left(\omega_o^2-\omega_p^2=\omega_p\Omega_c\cos\varepsilon\right)^{\frac{1}{2}}$$
$$\left[1-\frac{1}{2}\frac{\left(k_r^2+\omega_o^2/\omega_{E^r}^2\right)}{k^2}\sin^2\varepsilon-\frac{k_z^2}{k^2}\cos^2\varepsilon\right]\exp\left[\frac{1}{2}\left(\frac{\omega_o}{kV_e}\right)^2\right] \tag{36}$$

where $k=\left(k_r^2+k_z^2+\omega_o^2/\left(\omega_{E^r}^2\right)\right)^{\frac{1}{2}}$ and

$$\omega_o^2=\omega_p^2+3k^2V_e^2+\left(\Omega_c^2/k^2\right)\left(k_r^2+\omega_o^2/\omega_{E^r}^2\right).$$

Equation (36) gives the bremsstrahlung power per unit volume emitted into a unit solid angle (ergs/s cm^3 sr).

We will consider the backscattering case and assign the following values:

$$V_e/c = 1.2 \times 10^{-2} \; (T_e \approx 35 \text{ eV})$$

$$\Omega_o = 5.6 \times 10^{12} \text{ Hz} \; (\lambda = 337\mu)$$

$$\Omega_c = 3.5 \times 10^{10} \text{ Hz} \; (B_o = 2\text{kG})$$

and we look at right angles to the plasma cylinder ($\phi = 90°$). Thus, Eq. (36) becomes (using P in place of $dI/d\Omega$):

$$P \approx \frac{(2)^{\frac{1}{2}} e^2 \omega_p^{\,2} \left(\delta/(1-\delta)\right) V_e^{\,4}}{8c^3 (2\pi)^4 V_E \omega_E R_o} \int \frac{k dk_r \, dk_z}{\omega_o} \left(\omega_o^{\,2} - \omega_p^{\,2}\right)^{\frac{1}{2}}$$

$$\left[1 - \frac{1}{2} \frac{\left(k_r^{\,2} + \omega_o^{\,2}/\omega_E^{\,2} R_o^{\,2}\right)}{k^2}\right] \tag{37}$$

$$\exp\left[\frac{1}{2}(\omega_o/kV_e)^2\right] \; .$$

We make use of the following set of relationships and definitions in evaluating P:

$$k^2 = k_r^{\,2} + k_z^{\,2} + \omega_o^{\,2}/\omega_E^{\,2} R_o^{\,2}$$

$$\omega_o^{\,2} = \omega_p^{\,2} + 3k^2 V_e^{\,2} + \Omega_c^{\,2} (1 - k_z^{\,2}/k^2)$$

$$A \equiv \omega_E R_o / V_e$$

$$y \equiv k_r / k_D$$

$$z \equiv k_z / k_D$$

$$K \equiv k/k_D$$

$$k_D \equiv \omega_p/V_e$$

$$B^2 \equiv \Omega_c{}^2/\omega_p{}^2 \qquad (38)$$

$$C^2 \equiv \omega_o{}^2/\omega_p{}^2$$

to get:

$$K^2 = y^2 + z^2 + C^2/A^2 ;$$

$$C^2 = 1 + 3K^2 + B^2 (1 - z^2/K^2); \text{ and} \qquad (39)$$

$$B^2 = \frac{\Omega_c{}^2 C^2}{4A^2 (V_e/c)^2 \Omega_o{}^2}$$

We now have:

$$P \approx \frac{e^2 \left(\delta/(1-\delta)\right) \left(V_e/c\right)^5 \Omega_o{}^5}{2^{5/2} c^3 \pi^4 V_E} \frac{(A^2-3)^{5/2}}{A} \text{ Int.} \qquad (40)$$

where the dimensionless integral is:

$$\text{Int} = \int_0^{(3)^{-\frac{1}{2}}} dy \int_0^{(3)^{-\frac{1}{2}}} dz\, K(1-C^{-2})^{\frac{1}{2}} (1 + z^2/K^2) \exp(C^2/2K^2) . \qquad (41)$$

This double integral is evaluated by a multiple integration routine written for PL/I by C. V. Bitterli (Ref. 21).

For our particular case, we find B = 0.1302 C/A and the bremsstrahlung is given by:

$$P \approx 5.895 \times 10^{-22} \frac{(A^2-3)^{5/2}}{A} \text{ Int} \qquad (\text{watts/cm}^3 \text{ sr}) . \qquad (42)$$

Nonmagnetic Wave-Wave Bremsstrahlung

Our starting point is Eq. (43) from Tidman and Dupree (Ref. 4). That is:

$$P \approx \frac{e^2 \omega_p^2 (3)^{\frac{1}{2}} V_e}{3\pi^2 c^3} \int_0^{k_D} k^2 dk \, \frac{F_e(\omega_p/k)}{|F_e'(\omega_p/k)|} \qquad (43)$$

This equation was derived for isotropic distributions. We will, however, replace k_θ by k to obtain an estimate of the maximum amount of bremsstrahlung. As before, we can approximate the $F_e/|F_e'|$ term in Eq. (43) by an appropriate delta function since it goes through a resonance. Thus, we find in analogy to Eq. (35) and with $k_\theta \to k$, that we can approximate as follows:

$$\frac{F_e(\omega_p/k)}{|F_e'(\omega_p/k)|} \approx \frac{\delta}{(1-\delta)} \frac{k}{\omega_p} \frac{V_e^3}{V_E} \exp(\omega_p^2/2k^2 V_e^2) \frac{(2)^{\frac{1}{2}} k V_e}{\omega_E R_o} \delta(k-k_o) , \quad (44)$$

where $k_o = \omega_p/\omega_E R_o$. Thus P becomes:

$$P \approx \frac{e^2 \omega_p (2/3)^{\frac{1}{2}} V_e^5 (\delta/(1-\delta))}{\pi^2 c^3 V_E \omega_E R_o} \int_0^{k_D} k^4 \, dk \exp\left(\omega_p^2/2k^2 V_e^2\right) \delta(k-k_o) . \qquad (45)$$

We evaluate Eq. (45) to find:

$$P \approx \frac{(2/3)^{\frac{1}{2}} e^2 \omega_p^5 (\delta/(1-\delta))}{\pi^2 c^3 V_E} A^{-5} \exp(A^2/2), \qquad (46)$$

where as before $A = V_d/V_e$. Finally, making use of Eq. (31) we have:

$$P \approx \frac{32(2/3)^{\frac{1}{2}} e^2 (V_e/c)^5 \Omega_o^5 (\delta/(1-\delta))}{\pi^2 c^3 V_E} A^{-5}(A^2-3)^{5/2} \exp(A^2/2). \qquad (47)$$

Calculation of values (as given in Table 1) verifies Tidman's statement (Ref. 22) that the magnetic field is "of secondary importance in computing the bremsstrahlung at frequencies $\omega \approx 0$ (ω_e) $>> \Omega = eB/mc$." Thus, we find that, in our case, the magnetic wave-wave bremsstrahlung is down (to within a factor of 10) by Ω_c^2/ω_p^2 ($\approx 2 \times 10^{-4}$) compared with the maximum nonmagnetic wave-wave bremsstrahlung.

Table 1

Bremsstrahlung versus Scattered Power

(all values in watts/cm^3 sr)

A	$P_{free\text{-}free}$	P_{mag}	P_{nonmag}	P_s
8	9.71×10^{-4}	2.56×10^{-9}	4.77×10^{-6}	1.77×10^{-5}
9	1.59×10^{-3}	1.17×10^{-5}	8.91×10^{-3}	3.20×10^{-2}
10	2.46×10^{-3}	1.28×10^{-1}	3.29×10^{2}	1.16×10^{3}

Comparison with Scattered Power

The scattered power (P_s) per unit solid angle and per unit volume of illuminated plasma is:

$$P_s = F_o n_o \sigma_t , \tag{48}$$

where F_o is the incident power per unit area and σ_t is our previously calculated cross section (per unit solid angle). Since we are considering large values of A, we can use Eq. (26) for σ_t. Considering the backscattering case for simplicity, we have:

$$P_s \approx \frac{2F_o n_o \Omega_o^2 r_o^2 V_e^3 \delta}{V_E \omega_p^2 c^2 (1-\delta)} \exp(A^2/2) \tag{49}$$

Thus when we compare the four types of radiation as functions of A in Table 1, we can see the power emitted by the free-free bremsstrahlung (this is the conventional usage of the word "bremsstrahlung"), the magnetic wave-wave bremsstrahlung, the nonmagnetic wave-wave bremsstrahlung ($P_{nonmag} = I_{\omega_p}/4\pi$), and the scattered power. These are in watts/cm^3 sr and the scattered power is calculated assuming a typical F_o of 10 watts/cm^2.

We find that if $A > 8$, then an F_o of 10 watts/cm^2 should be adequate. However, there are some other factors which would tend to require a larger F_o. The bremsstrahlung is being generated in the bulk of the plasma, whereas the scattered radiation is emitted only from the small illuminated volume. Thus, a well collimated detecting system is needed to eliminate most of this stray bremsstrahlung. (On a considerably lower power level, the illuminated volume of plasma is itself immersed in bremsstrahlung from the surrounding plasma and part of this incident radiation would also be scattered into the receiver.)

Clearly, the real concern is the amount by which the plasma is nonthermal, as evidenced by the magnitude of A. In the case studied for the small illuminated volume, if A is less than 8, then the free-free bremsstrahlung will dominate since it does not decrease for $\omega > 2\omega_p$ as do the wave-wave varieties.

If Ω_o is too close to ω_p, then the enhanced scattering will decrease and bremsstrahlung will again dominate. In other words, the closer Ω_o is to ω_p, the larger A would have to be to generate a detectable scattered signal. When $\Omega_o \approx \omega_p$, V_d would have to be about c/3 or greater for resonance. (As mentioned in the discussion on forward scattering, V_d is very unlikely to become this large and our treatment is nonrelativistic.)

7. FURTHER COMPUTER STUDIES

Additional computer studies were carried out to give experimental workers more concrete information. Volume integrations were made along the path of the laser beam so that the total scattered power could be calculated. This scattered power was then compared to that generated by bremsstrahlung, also taken over the appropriate plasma volume. Various operating parameters were varied to determine their effect on the results. Finally, the scattered power and bremsstrahlung were calculated as functions of wavelength to determine if narrow-banding the receiver would help to improve the signal-to-noise ratio.

Volume Integrated Scattered Power

The laser beam enters the plasma along a chord located a distance R_o from the axis and is scattered into the receiver (Fig. 5). For simplicity, we will consider the incident laser beam to have a square cross section 1 centimeter on each side. Thus, the volume integration uses coordinates along the chord, perpendicular to the chord from R_o - 0.5 cm to R_o + 0.5 cm, and perpendicular to the chord in the z direction. The plasma is taken as uniform in the z direction (i.e., we are illuminating the center section), and the z coordinate contributes a simple multiplicative factor (in this case unity).

The density profile across the plasma is given by Eq. (21). The incident laser beam is perpendicular to the B_z guide field and the receiver is also located in the same x-y plane perpendicular to the magnetic field. All the internal parameters in the computer program, such as plasma density difference wave vector, $\vec{k}$, and its theta component, k_θ, are cast in terms of the two coordinates (along the chord and perpendicular to the chord in the x-y plane). The resultant volume double integral is then evaluated by the aforementioned routine written by C. V. Bitterli (Ref. 21).

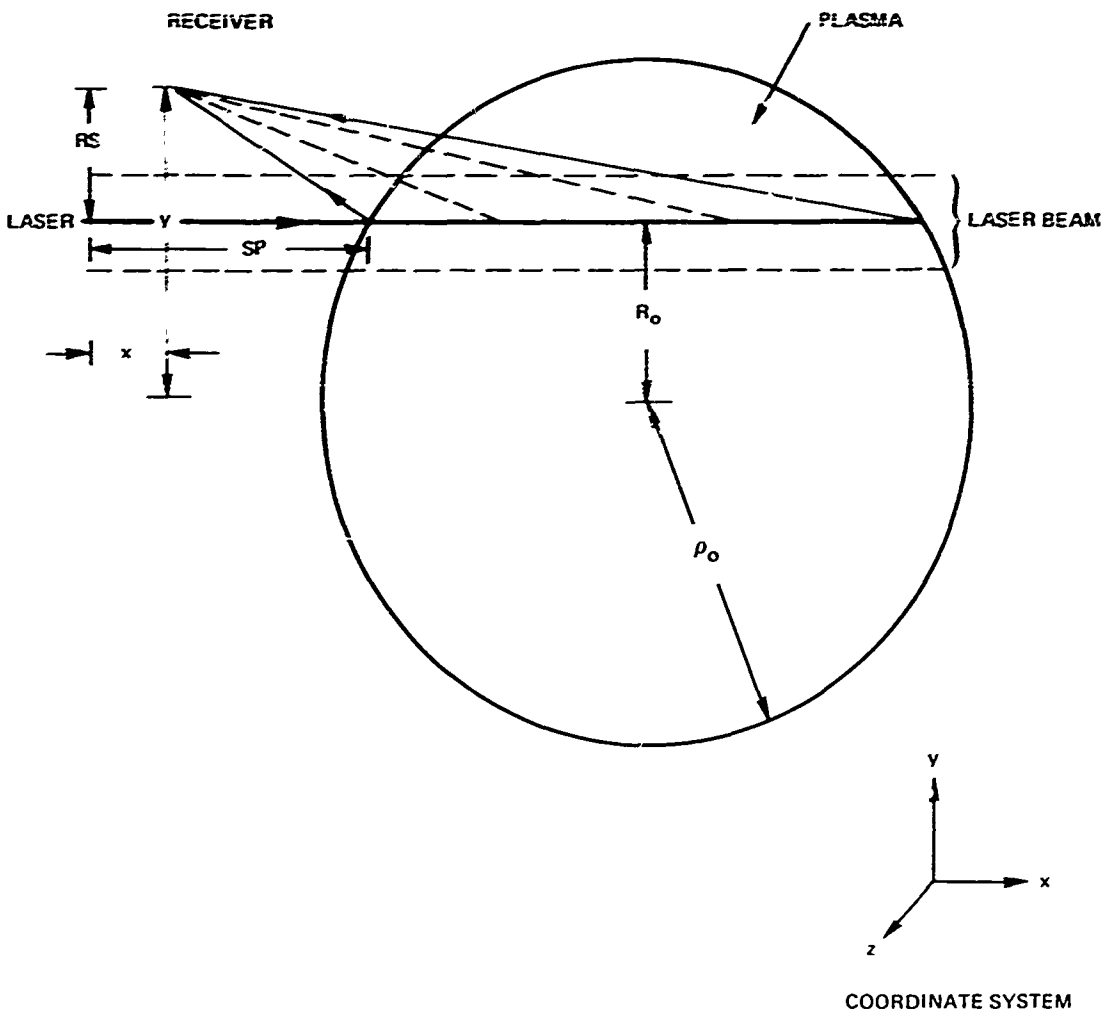

Fig. 5 SOURCE–RECEIVER ARRANGEMENT

A sample or typical run is given in Tables 2 and 3. In Table 2, we list the starting parameters of the computer run. In Table 3, we list the results of varying most of these parameters one by one as all the other parameters are kept at their initial values. We note that the maximum scattered power obtained in this particular run is 3.01×10^{-6} watts/steradian.

In another typical run, the starting parameters referred to in Table 2 became (in the same order) 2×10^{15} cm^{-3}, 1.6 cm, 2.3 cm, 3.1 cm, 1.2 cm, 5×10^{12} rad/s, 3.0 cm, 1.6 cm, 1.4×10^{11} rad/s, 10^{-6}, 0.1, 0.01, 10 watts/cm^2, 20 eV, and 10. The maximum scattered power for variations in λ, R_o, and SP were all down by about a factor of 10; all in all, there were no striking differences.

Volume Integrated Free-Free Bremsstrahlung

The bremsstrahlung entering the receiver comes, of course, not just from the volume of plasma illuminated by the laser beam, but from all the plasma subtended by the receiver aperture (Fig. 6, shaded area). For simplicity, this aperture is defined by the laser path length in the plasma (see Figs. 5 and 6).

A computer calculation using the Table 2 parameters yields a value for the free-free bremsstrahlung of 7.56×10^{-2} watts/sr. A similar run with R_o changed from 2.2 cm to 1.0 cm results in a value of 4.64×10^{-2} watts/sr. As expected, bremsstrahlung output is very sensitive to the plasma density. For example, changing the maximum density (n_o) to 2×10^{15} cm^{-3} leads to a result of 1.62 watts/sr, a significant increase. Thus, we see that in this case the free-free bremsstrahlung is at least four orders of magnitude stronger than the scattered signal. We note that this is for a wideband receiver, i.e., we have integrated over all frequencies.

Table 2

Starting Parameters for a Typical Computer Run

Parameter	Remarks	Initial Value
n_o	Maximum density	10^{15} cm^{-3}
r_o	Characteristic plasma dimension	1.27 cm
r_1	Maximum density radius	2.2 cm
ρ_o	Plasma radius	3.11 cm
R_o	Chord distance from axis	2.2 cm
Ω_o	Laser frequency	5.6×10^{12} rad/s
SP	Source distance to edge of plasma	4.0 cm
RS	Receiver distance to source	0.42 cm
Ω_c	Cyclotron frequency	3.5×10^{10} rad/s
γ	Fraction of nonthermal electron	10^{-6}
V_e/V_E	Ratio of thermal velocities	0.1
ω_e/ω_E	Ratio of drift frequencies	0.01
F_o	Laser power density	10 watts/cm^2
T	Temperature	35 e V
V_d/V_e	Ratio of drift velocity to thermal	10

Table 3

Scattered Power versus Parameter Variation for a Typical Run

Parameter	Range*	Scattered Power at Listed Range		Maximum Power within Parameter Range
		Lower	Upper	
r_o	1.55 to 1.65	1.49×10^{-8}	2.99×10^{-8}	1.85×10^{-7}
r_1	2.25 to 2.35	4.71×10^{-8}	1.37×10^{-8}	1.35×10^{-7}
R_o	1.00 to 1.30	9.38×10^{-9}	1.74×10^{-8}	5.83×10^{-7}
Ω_o	5.6×10^{12} to 4.6×10^{12}	2.70×10^{-8}	7.61×10^{-8}	7.61×10^{-8}
SP	2.80 to 3.20	5.57×10^{-8}	1.15×10^{-7}	3.01×10^{-6}
RS	1.55 to 1.65	1.14×10^{-7}	1.82×10^{-8}	3.21×10^{-7}
Ω_c	7×10^{10} to 7×10^{11}	1.13×10^{-7}	2.35×10^{-8}	1.13×10^{-7}
V_e/V_E	10^{-1} to 3.4×10^{-2}	2.70×10^{-8}	2.39×10^{-7}	2.39×10^{-7}
τ	35 to 15	2.70×10^{-8}	3.28×10^{-8}	2.70×10^{-8}
V_d/V_e	10 to 15	2.70×10^{-8}	2.25×10^{-9}	2.70×10^{-8}

*Each parameter is reset to its Table 2 value when other parameters are varied.

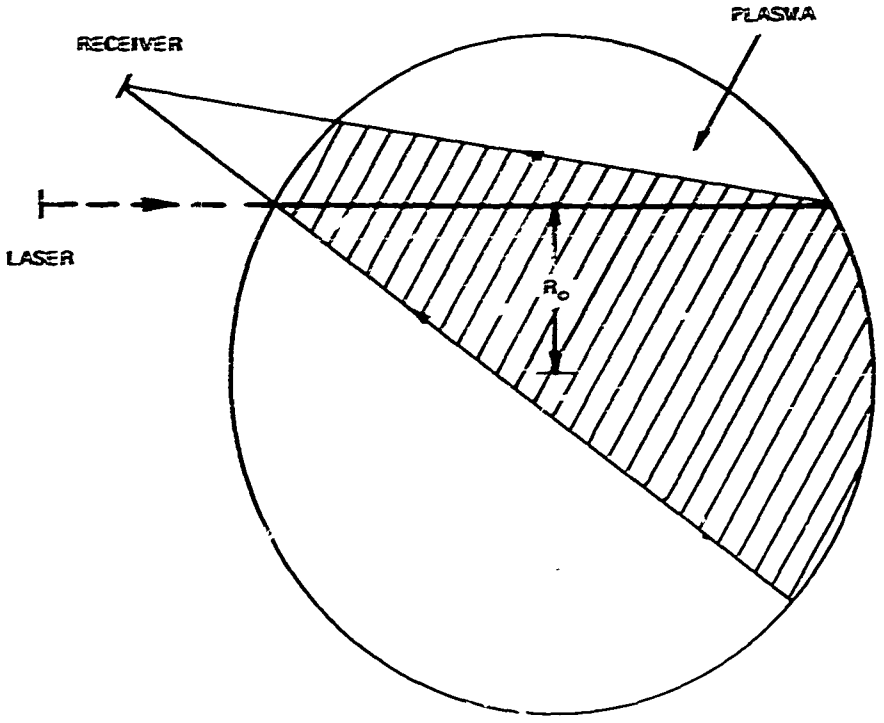

Fig. 6 BREMSSTRAHLUNG SEEN BY RECEIVER

Volume Integrated Wave-Wave Bremsstrahlung

Our starting point is Eq. (43) and we use Eq. (23) to determine the $F_e / |Fe'|$ part of the integral in Eq. (43). Once again, we replace k_θ by k to obtain an estimate of the maximum bremsstrahlung. We find that the wave-wave bremsstrahlung per unit volume and per unit solid angle is:

$$P \propto \frac{e^2 \omega_p^2 \nu_e}{(2\pi)^3 \tau^2 c^3} \int_0^{\infty} D \epsilon^2 d\epsilon$$

$$\left\{ \frac{\frac{4(1-\delta)}{(2\pi)^3 \nu_e} \exp\left[-\frac{1}{2\nu_e^2}\left(\frac{\omega_p}{\epsilon} - \omega_{e'}\right)^2\right] - \frac{\delta}{(2\pi)^3 \nu_\Sigma} \exp\left[-\frac{1}{2\nu_\Sigma^2}\left(\frac{\omega_p}{\epsilon} - \omega_{\Sigma'}\right)^2\right]}{\left|\frac{4(1-\delta)}{(2\pi)^3 \nu_e^3}\left(\frac{\omega_p}{\epsilon} - \omega_{e'}\right) \exp\left[-\frac{1}{2\nu_e^2}\left(\frac{\omega_p}{\epsilon} - \omega_{e'}\right)^2\right] - \frac{\delta}{(2\pi)^3 \nu_\Sigma^3}\left(\frac{\omega_p}{\epsilon} - \omega_{\Sigma'}\right) \exp\left[-\frac{1}{2\nu_\Sigma^2}\left(\frac{\omega_p}{\epsilon} - \omega_{\Sigma'}\right)^2\right]\right|} \right\} \quad (59)$$

The multiple integration routine used earlier (Ref. 21) gives us the results for the triple integral involved in summing across the plasma.

The result for the Table 2 parameters is 6.03 watts/sr. We see, therefore, that for this particular plasma, the wave-wave bremsstrahlung dominates both the free-free bremsstrahlung and especially, the scattered signal.

Thus, the dominance of bremsstrahlung as indicated above leads us to look at the frequency (or wavelength) dependence to see if narrow-banding the receiver would help.

Free-Free Bremsstrahlung versus Wavelength

The free-free bremsstrahlung is very easy to handle. A typical reference such as Glasstone and Lovberg provided us with the necessary formula (Ref. 19, p 32). Although the bremsstrahlung and scattered signal shall be listed as functions of wavelength in microns for convenience,

in units they are in watts/sr Hz. As expected, the bremsstrahlung is essentially uniform from 10μ to 447μ at 1.01×10^{-19} watts/sr Hz.

Scattered Power versus Wavelength

The scattered signal case is more involved. We use some of our basic theory formulas that do not involve integrations over frequency. Recalling Eq. (11), we have:

$$S_{se}(\vec{k},\omega) = \frac{\left(\frac{2\pi}{k}\right) F_c\,(-\vec{k},\,\omega/k)}{\left(1 - \frac{\omega_p^2}{\omega^2} - \frac{3k^2V_e^2\omega_p^2}{\omega^4} - \frac{\omega_p^2}{\omega^4}\frac{\Omega_c^2k^2}{k^2}\right)^2 + \frac{\pi^2\omega_p^4}{k^4}\left[F_e'\,(-\vec{k},\,\omega/k)\right]^2} \tag{51}$$

The differential cross section per unit solid angle and per unit frequency interval then becomes (for scattering perpendicular to the magnetic field direction):

$$\sigma = \frac{\left(\frac{r_o^2 2\pi}{k}\right) F_e\left(\frac{\omega}{c}\vec{N}-\vec{K},\,\frac{\omega-\Omega_o}{|\vec{K}-\frac{\omega}{c}\vec{N}|}\right)}{\left[1 - \left(\frac{\omega_p}{\omega-\Omega_o}\right)^2 - \frac{3k^2V_e^2\omega_p^2}{(\omega-\Omega_o)^4} - \frac{\omega_p^2\Omega_c^2}{(\omega-\Omega_o)^4}\right]^2 + \frac{\pi^2\omega_p^4}{k^4}\left[F_e'\left(\frac{\omega}{k}\vec{N}-\vec{K},\frac{\omega-\Omega_o}{|\vec{k}-\frac{\omega}{c}\vec{N}|}\right)\right]^2} \tag{52}$$

Several computer runs were made using Eq. (52) and the bi-Maxwellian given before (Eqs. (20) and (22)). The receiver position with respect to the source was varied by changing the x and y coordinates (see Fig. 5). The results, listed in Table 4, show that it is possible in principle to achieve scattering signals above the free-free bremsstrahlung for receiver wavelengths around 457μ for the 10 watts/cm^2 laser power density that we are using. Thus narrow-banding the receiver does help to narrow the gap between the scattered signal and the free-free bremsstrahlung. In general, we note that the backscattering cases give stronger scattered signals. When the receiver was moved towards the forward scattering position, the wavelength at which the peak signal was received tended (in some cases) to be shorter.

Wave-Wave Bremsstrahlung versus Wavelength

The next step is to determine the magnitude and wavelength (really frequency) dependence of the wave-wave bremsstrahlung. Once again we turn to Tidman and Dupree (Ref. 4) and, using their Eqs. (17), (13), (12), and (40), we find that:

$$\frac{dP}{d\omega} \approx \frac{e_2\,\omega_p^4}{6\pi^3 c^3 \omega} \left(\omega^2 - \omega_p^2\right)^{\frac{1}{2}} \int_0^{k_D} dk\, S_{ee}(\vec{k}, \omega) \tag{53}$$

We use Eq. (51) for S_{ee} to obtain:

$$\frac{dP}{d\omega} \approx \frac{e^2\,\omega_p^4}{3\pi^2 c^3 \omega} \left(\omega^2 - \omega_p^2\right)^{\frac{1}{2}} \int_0^{k_D} \frac{dk}{k} \cdot$$

$$\frac{F_c(-\vec{k},\ \omega/k)}{\left\{\left(1 - \frac{\omega_p^2}{\omega^2} - \frac{3k^2 V_c^2 \omega_p^2}{\omega^4} - \frac{\omega_p^2 \Omega_c^2}{\omega^4}\right)^2 + \frac{\pi^2 \omega_p^4}{k^4} \left[F_c'(-\vec{k},\ \omega/k)\right]^2\right\}} \tag{54}$$

Table 4

Scattered Power versus Wavelength for Different Receiver Positions

λmin	λmax	x	y	P(λmin)	P(λmax)	Max P	at λ
97	527	0	3.2	1.50×10^{-34}	2.10×10^{-26}	4.42×10^{-21}	457
97	527	1.0	3.2	1.62×10^{-34}	2.09×10^{-26}	9.64×10^{-21}	457
97	527	2.0	3.2	1.85×10^{-34}	2.06×10^{-26}	2.36×10^{-19}	457
97	527	3.0	3.2	2.37×10^{-34}	2.02×10^{-26}	5.95×10^{-21}	457
97	527	4.0	3.2	3.59×10^{-34}	1.97×10^{-26}	4.97×10^{-22}	457
97	527	5.0	3.2	2.92×10^{-34}	1.65×10^{-26}	1.04×10^{-22}	477
97	527	6.0	3.2	1.50×10^{-34}	1.00×10^{-26}	2.26×10^{-22}	427
97	527	7.0	3.2	1.66×10^{-34}	3.57×10^{-27}	8.44×10^{-24}	327
97	527	8.0	3.2	1.08×10^{-34}	4.79×10^{-28}	6.68×10^{-22}	287
97	527	9.0	3.2	7.25×10^{-34}	1.16×10^{-29}	2.60×10^{-23}	447
97	527	10.0	3.2	1.90×10^{-37}	7.60×10^{-32}	8.56×10^{-26}	257
227	527	0	2.6	1.66×10^{-28}	2.14×10^{-26}	1.69×10^{-21}	457
227	527	7.0	2.6	9.14×10^{-29}	3.96×10^{-27}	1.80×10^{-23}	267
447	467	0	2.6	4.58×10^{-23}	5.05×10^{-25}	2.88×10^{-21}	464.6

where we are again considering radiation emitted perpendicular to the magnetic field.

Equation (54) is our basic equation and the result of using it in the computer calculation is, as expected, a monotonic decrease in power from the longer to the shorter wavelengths. Thus, at $\lambda = 527\mu$ (closest to a typical λ_p of 1110) the output is 5.85×10^{-14} watts/sr Hz, whereas at $\lambda = 97\mu$ the output has decreased to 6.34×10^{-21} watts/sr Hz. At 457μ, the wave-wave bremsstrahlung is 1.78×10^{-14}, or five orders of magnitude above the scattered signal. Thus we see that narrow-banding the receiver does help with the free-free bremsstrahlung which is frequency independent in this regime. Narrow-banding does not help, however, with the wave-wave bremsstrahlung, since the same mechanism is at work generating both it and the enhanced scattering cross section at all wavelengths. Approximately the same ratio then exists between the wideband frequency-integrated (i.e., independent) scattered signal and frequency-integrated wave-wave bremsstrahlung as between their frequency-dependent counterparts.

This leads us naturally into the next section, where we shall consider lasers whose Ω_o are much greater than ω_p.

Results for CO_2 and Ruby Lasers

Some runs were made using CO_2 and ruby laser wavelengths, 10.6μ and 0.694μ, respectively. The other parameters were as given in Table 1, except RS (Receiver distance to Source) which was changed slightly from 0.42 cm to 0.40 cm. Some typical results were 1.50×10^{-20} watts/sr Hz at 10.4μ and 1.87×10^{-20} at 10.8μ. At ruby laser wavelengths, we found 1.72×10^{-22} watts/sr Hz at 0.69μ and 9.12×10^{-22} at 0.595μ.

Thus, the CO_2 laser at 10.6μ provides a scattering signal that is comparable to or slightly better than that generated by the far-infrared 337μ laser. The CO_2 laser,

moreover, can provide a power density many orders of magnitude greater than the 10 watts/cm^2 typical of the HCN laser. The CO_2 laser, therefore, would seem to be a good candidate for use in an enhanced scattering experiment.

The ruby laser is also a possibility but at a scattering power level about 2 orders of magnitude less than that for the CO_2 laser. Thus, for similar results, the ruby laser must be about 100 times more powerful than the corresponding CO_2 laser.

Finally, we see that for the plasmas being considered, these lasers have the advantage that $\Omega_o >> \omega_p$. This means that we do not have to worry about the anomalous or wave-wave bremsstrahlung. For example, at 10.4μ the wave-wave bremsstrahlung is down to the negligible level of 1.6×10^{-49} watts/sr Hz.

8. SUMMARY AND CONCLUSIONS

We have investigated the conditions under which enhanced scattering can be obtained from theta-pinch-type plasmas.

We found that a necessary, but not always sufficient, requirement for enhanced scattering is the presence of a nonthermal electron component in the plasma. These nonthermal electrons generate the high-amplitude electron density fluctuations that scatter the incoming radiation. The electron density fluctuations are manifestations of the high-energy plasma oscillations generated by the nonthermal electrons. When the difference wave vector and beat frequency between the incoming and outgoing radiation match the wave vector and frequency of the plasma oscillations, the scattering cross section is greatly enhanced (i.e., resonance occurs).

The theory was applied to theta-pinch-type plasmas via the rigid rotor model. It was found that resonance occurs when the difference wave vector k_θ equals ω_o/V_d.

The broadness of the scattering resonance and its sensitivity to various parameter changes were investigated. It was found that the resonance was wide enough to give substantial enhancement in the case studied. The ratio, A, of the drift velocity of the nonthermal electrons to the thermal velocity of the background is the critical parameter in the analytic studies, since it appears in the argument of exponential terms. For the case studied, it was found that the ratio needed to be 7 or over for significant enhancement.

We found that the backscattering case (i.e., as small an angle as is practical between source and receiver) was the most promising. The resonance condition was most

easily satisfied and, in geometries such as Fig. 4, a finite volume of the plasma would remain in resonance.

The most troublesome aspect of any enhanced scattering experiment is bremsstrahlung. For typical laser power densities of 10 watts/cm and considering the unit volume of illuminated plasma that is in resonance, we found that the drift velocity ratio A must be greater than 8 for the scattered power to be greater than the bremsstrahlung (Table 1). For $A \leq 8$, the conventional or free-free bremsstrahlung dominates. For $A \approx 9$ and greater, the major contribution to the bremsstrahlung comes from the anomalous or wave-wave variety.

In the computer studies, we calculated the actual scattered power and the two types of bremsstrahlung that would reach the receiver under typical conditions. The frequency integrated scattered power was found to be 4 orders of magnitude below the free-free bremsstrahlung and 6 orders of magnitude below the wave-wave bremsstrahlung for the case studied.

Narrow-banding the receiver and looking at these three quantities per frequency interval showed that the scattered power could be made more or less comparable to the free-free bremsstrahlung. In one special case (Table 4), which would probably be very difficult to attain experimentally, the scattered power was actually twice the free-free bremsstrahlung. The wave-wave bremsstrahlung, however, is still 5 orders of magnitude larger than the scattered signal.

Finally, we found that a CO_2 laser would be much more suitable for use with a narrowband receiver. The free-free bremsstrahlung is the same as before, the wave-wave bremsstrahlung is negligible around 10.6μ, and the scattering cross section is about the same as that for the 337μ or HCN laser. Since the CO_2 laser is much more powerful than the HCN laser, the prospects for a successful scattering experiment would seem to be good with the CO_2 laser.

REFERENCES

1. M. N. Rosenbluth and N. Rostoker, "Scattering of Electromagnetic Waves by a Nonequilibrium Plasma," Phys. Fluids, Vol. 5, 1962, p. 776.

2. F. Perkins and E. E. Saltpeter, "Enhancement of Plasma Density Fluctuations by Nonthermal Electrons," Phys. Rev., Vol. 139, 1965, p. A55.

3. D. C. Montgomery and D. A. Tidman, Plasma Kinetic Theory, McGraw-Hill Book Company, Inc., New York, 1964.

4. D. A. Tidman and T. H. Dupree, "Enhanced Bremsstrahlung from Plasmas Containing Nonthermal Electrons," Phys. Fluids, Vol. 8, 1965, p. 1860.

5. D. A. Tidman, T. J. Birmingham, and H. M. Stainer, "Line Splitting of Plasma Radiation and Solar Radio Outbursts," Astrophys. J., Vol. 146, 1966, p. 207.

6. J. P. Freidberg and R. L. Morse, "Z-Dependent Marginal Stability of the Rigid Rotor Model of a High Beta Theta-Pinch," presented at the Conference on Pulsed High-Density Plasmas of the American Physical Society, Los Alamos, New Mexico, 1967.

7. R. L. Morse, "Adiabatic Time Development of Linear Theta-Pinch Plasma Profiles," Phys. Fluids, Vol. 10, 1967, p. 1560.

8. R. L. Morse, Equilibria of Collisionless Plasma, Los Alamos Rpt. LA-3844-MS, 1968.

9. J. P. Freidberg and W. Grossmann, "Two-Dimensional Equilibrium for High-β Mirror Devices Including Particle Loss," Phys. Fluids, Vol. 11, 1968, p. 2476.

10. J. P. Freidberg and R. L. Morse, "Collisionless Tearing Mode Instabilities in a High-β Theta Pinch," Phys. Fluids, Vol. 12, 1969, p. 887.

11. J. P. Friedberg, private communication.

12. R. L. Morse and J. P. Freidberg, "Rigid Drift Model of High-Temperature Plasma Containment," Phys. Fluids, Vol. 13, 1970, p. 531.

13. E. G. Harris, "Comments on 'Rigid Drift Model of High Temperature Plasma Containment'," Phys. Fluids, Vol. 13, 1970, p. 2425.

14. A. N. Kaufman, "Resonant Interactions between Particles and Normal Modes in a Cylindrical Plasma," Phys. Fluids, Vol. 14, 1971, p. 387.

15. H. M. Stainer, "Rotational Effects in a High-Beta Plasma Confined by a Longitudinal Magnetic Field," Phys. Fluids, Vol. 13, 1970, p. 193.

16. N. N. Komarov and V. M. Fadeev, "Plasma in a Self-Consistent Magnetic Field," Zh. Eksp. Teor. Fiz., Vol. 41, 1961, p. 528 (Trans. in Sov. Phys. - JETP, Vol. 14, 1962, p. 378).

17. D. A. Tidman, "Enhanced Fluctuations in Plasmas," University of Maryland Technical Note BN-426, December 1965.

18. L. Spitzer, Jr., Physics of Fully Ionized Gases, Interscience Publishers, New York, 1962.

19. S. Glasstone and R. H. Lovberg, Controlled Thermonuclear Reactions, D. Van Nostrand Company, Inc., Princeton, 1960.

20. C. Chin-Fatt and H. R. Griem, "Enhanced Radiation from a Theta-Pinch Plasma," Phys. Rev. Ltrs., Vol. 25, No. 24, 1970, p. 1644.

21. C. V. Bitterli, "Multiple Integration (PL/I)," APL Computing Center Library Routine No. 5.01.10, January 1971.

22. D. A. Tidman, "Radio Emission from Shock Waves and Type II Solar Outbursts," J. Planet. Space Sci., Vol. 13, 1965, p. 781.

ACKNOWLEDGMENTS

This problem was suggested by A. M. Stone and was motivated by experimental work being conducted by R. Turner. The author acknowledges with thanks the many helpful discussions held with R. Turner. Helpful criticism was also received from E. P. Gray. The work was supported by the U.S. Navy under contract N00017-72-C-4401.

Preceding page blank

Appendix A

RESONANCE SPIKE

We wish to examine the conditions under which the denominator of the first term on the right hand of Eq. (25) can vanish. As before, we are considering only those cases where $bd \ll 1$ (the background plasma has a very small drift velocity). The physical limits of any considered experiment are such that b is near 1. In this case, we look for solutions of the form $b = 1 + \epsilon$ where ϵ is a very small number. We find that:

$$\epsilon \exp\left\{-\left[a\left(\frac{V_e}{V_E}\right)\epsilon\right]^2\right\} = \frac{(1-\delta)}{\delta}\left(\frac{V_E}{V_e}\right)^3 \exp(-a^2). \quad \text{(A-1)}$$

To a very good degree of approximation, we can write:

$$\epsilon = \frac{(1-\delta)}{\delta}\left(\frac{V_E}{V_e}\right)^3 \exp(-a^2). \quad \text{(A-2)}$$

For a typical case, where $\delta/(1-\delta) = 10^{-6}$, $V_E/V_e = 10$, and $a = 6$, the difference between (A-2) and an iteration starting with (A-2) and using (A-1) is in the 13th decimal place and $\epsilon = 2.3 \times 10^{-7}$. The parameter b was programmed as $1 + (1 \pm \Delta)\epsilon$ where Δ went as 0.01, 0.001, 0.0001, 0.00001, 0.000001, and 0 (zero). There was very little difference between the plus- and minus-sign cases, and the enhancement factor for the minus case went as 2.2×10^{10}, 2.2×10^{11}, 2.2×10^{12}, 2.2×10^{13}, 2.6×10^{14}, and 9.3×10^{14}, respectively. Thus, it can be seen that this spike is indeed very narrow.

Preceding page blank